JOURNAL OF SPACECRAFT AND ROCKETS
Vol. 36, No. 5, September–October 1999

Characteristics of an Anomalous Orbital Debris Population Inferred from Theoretical Modeling

R. Lambour* and R. Sridharan†
Lincoln Laboratory, Massachusetts Institute of Technology, Lexington, Massachusetts 02420-9185

We construct a low-fidelity thermal model to facilitate characterization of an anomalous orbital debris population believed to be NaK reactor coolant that leaked from the nuclear reactors of a now defunct class of Soviet Radar Ocean Reconnaissance Satellites. The model is used to assess the probable state of the debris; it is concluded that these debris are in the liquid state. This result is then applied to a low-fidelity evaporation model to assess whether evaporation causes a change in area to mass ratio on time scales equal to or shorter than the approximate orbital lifetime. It is concluded that the time scale for significant evaporation of the droplet is much longer than the orbital lifetime and that orbital lifetime is not significantly influenced by evaporation of the droplets.

Nomenclature

A_p = projected area of the debris, m^2
A_s = surface area, m^2
$a(b)$ = initial mass of Na (K) in NaK droplet, kg
C = specific heat of the debris, J/kg-K
E_{absorbed} = energy absorbed by the debris ($E_S + E_{\text{reflec}} + E_{\text{therm}}$)
E_{radiated} = thermal energy radiated by the debris, J
E_{reflec} = absorbed Earth-reflected solar energy, J
E_S = absorbed solar energy, J
E_{therm} = absorbed terrestrial thermal energy, J
F_S = solar energy flux at the Earth, 1360 W/m^2
F_{therm} = terrestrial thermal energy flux, W/m^2
h = altitude of the debris, km
M_i = molar weight of element i, kg/mole
m = mass of the debris, kg
N_i = mole fraction of element i
P = vapor pressure at temperature T, Pa
P_i^0 = vapor pressure for pure element i at temperature T, Pa
R = gas constant, 8.31 J/mol-K
R_E = radius of the Earth, 6378 km
r = radius of a debris object, m
T = temperature of the debris, K
t = time, s
W_i = evaporation rate of element i, kg/s
$x(y)$ = mass of evaporated Na (K), kg
α = absorptivity of NaK
β = half-angle subtended by the Earth at the debris altitude
γ_i = activity coefficient
ε = emissivity of NaK
θ = right ascension of ascending node
κ = evaporation coefficient, assumed equal to 1
ρ = density of eutectic NaK, kg/m^3
ρ_E = angular radius of the Earth viewed from the sun
σ = Stefan–Boltzmann constant, 5.67×10^{-8} W/m^2-K^4
ϕ = orbital inclination

Introduction

IN a companion paper,[1] we described a remote sensing effort carried out at the Massachusetts Institute of Technology Lincoln Laboratory, at the behest of NASA, to characterize constituents of an anomalous orbital debris population. The debris are termed anomalous because the detection rate of >0.6 cm debris far exceeded that predicted by orbital debris models and had orbital characteristics that were different from those expected from known debris sources. The only source found to be consistent with the observational data was liquid coolant that leaked from the nuclear reactors of a now defunct class of Soviet Radar Ocean Reconnaissance Satellites (RORSAT). The coolant is believed to have leaked after the reactor cores were separated from the spacecraft and boosted into disposal orbits located at ~65-deg inclination and 850–1000 km altitude.[2] The nuclear reactors used on the RORSATs are believed to be of the Bouk class, a slightly older design than the more familiar Topaz and Topaz-II.[3] The Bouk-class reactor utilized a liquid sodium-potassium alloy (NaK) of eutectic composition (77.8% K and 22.2% Na by weight) as coolant.‡

In Ref. 1, we used the Millstone Hill L-band radar to locate 11 objects from the anomalous debris population. These objects were found to be distributed in several orbit planes at ~65-deg inclination and 850–1000 km in altitude. Multiple objects were found in some of the orbit planes. Data from the Millstone Hill and Haystack radars, as well as from optical photometers and a charge-coupled device photopolarimeter, were used to infer the following properties about the debris. They are spherical in shape, highly reflective (reflectivity = 0.84–0.89), and have metallic surfaces. They range in radius from ~1.6 to 2.9 cm and have a mean density of 1.03 ± 0.05 g/cm^3. This density is consistent with the density of eutectic NaK at 300 K (0.868 g/cm^3) (Ref. 4), a nominal temperature for orbital debris. Although the optical properties of eutectic NaK are not known, these properties are consistent with the hypothesis that the anomalous debris are NaK coolant that leaked from the RORSAT power sources. The discovery of multiple debris per orbit plane is also suggestive of a leaking liquid.

In this paper, we develop a low-fidelity thermal model of the anomalous debris, using the properties inferred from the radar and optical observations, to assess whether the debris are in a liquid or solid state. The conclusion of this model is then applied to a low-fidelity evaporation model to assess whether the orbital lifetimes of the debris are significantly influenced by evaporation.

Time-Dependent Thermal Model for the Anomalous Debris

We have constructed a simple, time-dependent thermal model that is used to compute the temperature of the anomalous debris as it orbits the Earth. Using conservation of energy, the rate of change in

Received 10 March 1998; revision received 30 September 1998; accepted for publication 4 October 1998.

*Staff Member, Surveillance Techniques Group, 244 Wood Street.
†Senior Staff Member, Surveillance Techniques Group, 244 Wood Street. Member AIAA.

‡Russian Institute of Physics and Power Engineering Web site, http://www.rssi.ru/ippe/general/spacer.html.

temperature of a single debris object can be written in the following manner:

$$\frac{dT}{dt} = \frac{(E_{\text{absorbed}} - E_{\text{radiated}})}{Cm} \tag{1}$$

where the numerator represents the difference between the energy absorbed by the object and the energy radiated by the object, whereas the denominator represents the product of the specific heat C and the mass (also referred to as the thermal mass). Given an initial temperature, this differential equation can be solved numerically for the thermal history of the object.

The absorbed energy originates from multiple sources, the most important of which are the sun, Earth-reflected sunlight, and terrestrial long-wave radiation ($E_{\text{absorbed}} = E_S + E_{\text{reflec}} + E_{\text{therm}}$). The absorbed solar energy can be written as

$$E_S = F_S \alpha A_p \tag{2}$$

The anomalous debris are assumed spherical; therefore, $A_p = \pi r^2$. We make a gray-body approximation for α; i.e., α does not vary with wavelength.

The solar energy input is eliminated when the debris object is in eclipse. We determine when the debris object is in eclipse using the following method. Let $\boldsymbol{X}$ be a vector from the sun to the satellite, and $\boldsymbol{P}$ is a vector from the sun to the center of the Earth. The angular radius of the Earth as seen from the sun is

$$\rho_E = \arcsin(R_E/P) \tag{3}$$

The satellite will be in eclipse (behind the disk of the Earth) when

$$\rho_E > \arccos(\boldsymbol{P} \cdot \boldsymbol{X}), \qquad |\boldsymbol{X}| > |\boldsymbol{P}| \tag{4}$$

This geometry is shown in Fig. 1.

Earth-reflected sunlight can be described by an equation of the same form as Eq. (2). The energy flux of reflected sunlight depends on the altitude of the debris, the albedo of the Earth, and the illuminated surface area of the Earth visible to the object. This last quantity is related to the direction cosine of the position vector of the object, the solar position vector, and the altitude the object[5] (Fig. 2). We have digitized the quantities presented in Fig. 3 of Ref. 5 and use these quantities as a look-up table to determine the Earth-reflected solar flux. These quantities are reproduced in Fig. 3. For example, at 1000-km altitude and a globally averaged albedo of 0.34, the reflected solar flux is ~450 W/m^2. This look-up table can be scaled to any globally averaged albedo.

The terrestrial long-wave radiation input is represented by

$$E_{\text{therm}} = F_{\text{therm}} \alpha A_p \tag{5}$$

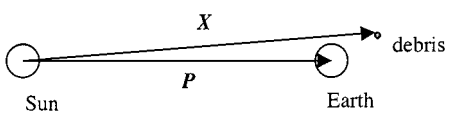

Fig. 1 Geometry used to determine whether debris is in eclipse.

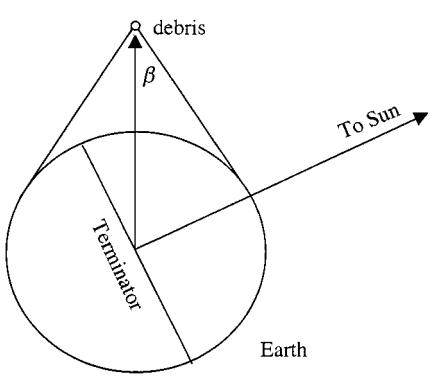

Fig. 2 Surface area of the Earth visible to a debris object at altitude h and the relation between the debris and solar position vectors.

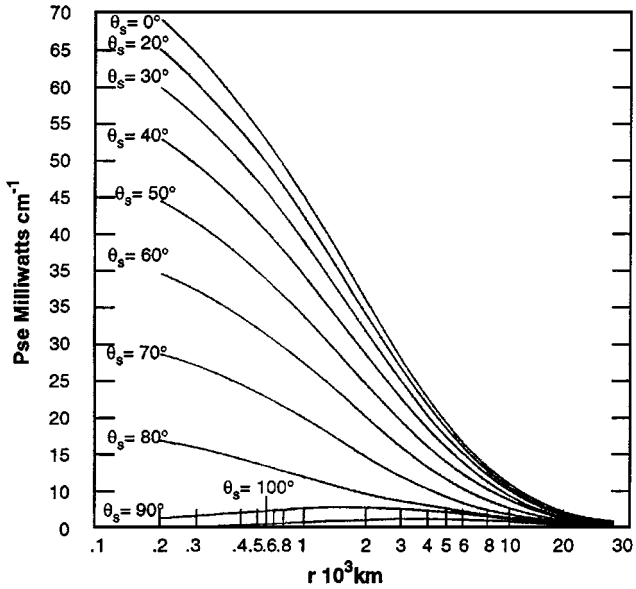

Fig. 3 Earth-reflected solar power input per unit cross-sectional area for a spherical satellite as a function of altitude, where angle θ_s is the angle between the debris and solar position vectors. Adapted from Ref. 5.

The thermal energy flux is taken to be 238 W/m^2 at the surface of the Earth, which is a global average and assumes that the Earth is a diffuse radiator.[6,7]

To determine the radiated energy, we assume that the object radiates as a blackbody. Then, the energy radiated to free space can be written as

$$E_{\text{radiated}} = \sigma \varepsilon T^4 A_s \tag{6}$$

The surface area is taken as $4\pi r^2$. We assume that ε does not vary with wavelength. The radiated energy is affected by the proximity of the warm Earth. This reduces the area of the sphere radiating to free space by a factor of Ωr^2, where $\Omega = 2\pi[1 - \cos(\beta)]$. At the altitude of the sphere h, the Earth subtends a half-angle:

$$\beta = \sin^{-1}[r/(r + h)] \tag{7}$$

We assume that the anomalous debris consist of eutectic NaK and are spherical in shape. The specific heat and density of eutectic NaK were determined using data from standard engineering tables.[4,8] The data were plotted and then fit to functions to extrapolate the quantities down to the freezing point of eutectic NaK (260.85 K). The specific heat is represented by

$$C(T) = 1112.19 - 0.608T + 0.000384T^2 \tag{8}$$

and the density is represented by

$$\rho(T) = 940.6 - 0.241T \tag{9}$$

As the temperature of the droplet varies, these quantities change. The mass of the droplet is assumed to remain constant.

The optical properties of NaK are not well known. Unpublished work by Russian researchers indicates that the absorptivity and emissivity coefficients of the material are believed to be roughly 0.156 and 0.132, respectively. We believe the value for the absorptivity of the material is reasonable because of the radar and optical characterization work carried out at Lincoln Laboratory, the optical work of Russian researchers, and previously published work.[1,9,10] The anomalous debris were shown to be metallic, highly reflective, and have a low optical polarization ratios.[1] Based on these data, it is not likely that debris are transparent; therefore, the reflectivity and absorptivity coefficients should sum to 1.0. The reflectivity values of 0.84–0.89 then lend credibility to the absorptivity value of 0.156. No such verification exists for the emissivity value. However, the emissivity values for liquid sodium and liquid potassium are generally low at the temperatures expected on orbit. The total normal emissivity of liquid sodium is on the order of 0.01–0.05 at ~300 K (Refs. 11 and 12). The value for liquid potassium is ~0.01 at ~300 K

(Ref. 13). These values are significantly lower than value reported for NaK (0.132). Nevertheless, we assume that the values $\alpha = 0.156$ and $\varepsilon = 0.132$ apply to NaK and discuss the effects of varying them in a later section.

To determine the motion of the debris and its effect on the absorbed and emitted radiation, we specify the orbit plane of the debris object with respect to an inertial reference frame. This reference frame is centered on the Earth and has its x axis pointing toward the sun, its z axis aligned with the rotation axis of the Earth, and $y = z \times x$. We also assume that the axial tilt of the Earth with respect to the ecliptic plane is 0 deg. The debris orbit plane is specified by the inclination of the orbit and the local-time location of the ascending node (see the Appendix). The initial position of the debris object is assumed to be the ascending node. Because the orbit of the debris object is assumed to be circular, the position of the debris in its orbital plane is easily computed. The debris position vector is then rotated into the reference frame, and the energy input and loss are calculated, resulting in a temperature change (dT/dt) for the time step. The temperature is adjusted, and the next step is taken. The initial temperature for the debris was arbitrarily chosen as 285 K. We considered other initial temperatures and found that they had no effect on the conclusion of this paper.

Predicted Thermal Behavior of the Anomalous Debris

We have applied the thermal model to several hypothetical debris pieces and orbits to understand how the various components of the model affect the debris temperature. We then applied the model to the actual debris and orbits presented in Ref. 1. We shall discuss the results from each application in turn. For the hypothetical case, we selected two droplet masses for consideration: 57 and 1 g. The larger (smaller) mass corresponds to a sphere with radius 2.5 cm (6.5 mm) at 285 K and roughly cover the proposed size range for these debris.[1] The orbits were assumed to be circular and had an inclination of 65 deg. For this inclination and altitude, the right ascension of the ascending node will precess through all values in a few months. However, for this calculation, we held the right ascension constant at three representative values. The altitude is also allowed to vary between 850 and 1000 km. The results for both spheres at an altitude of 925 km are shown in Fig. 4. Both Figs. 4a and 4b show three

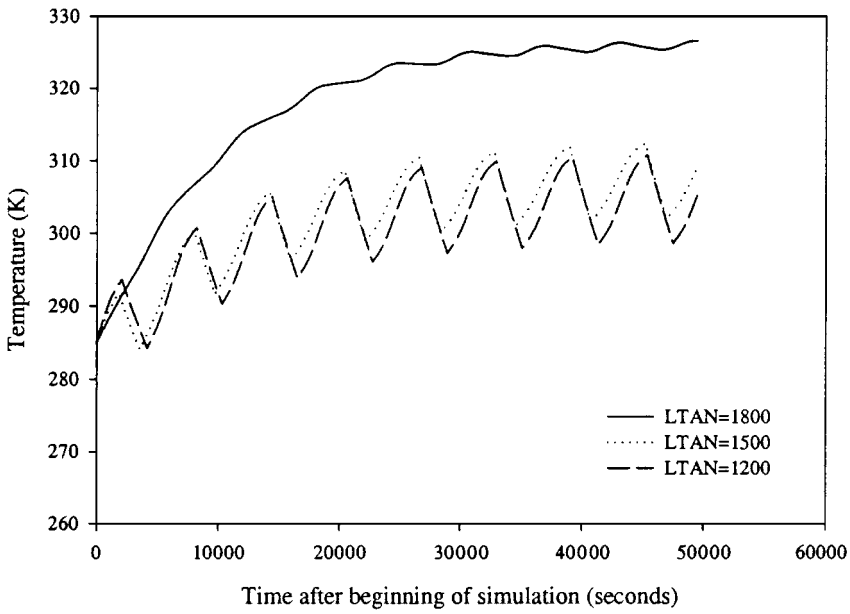

a) 57-g sphere

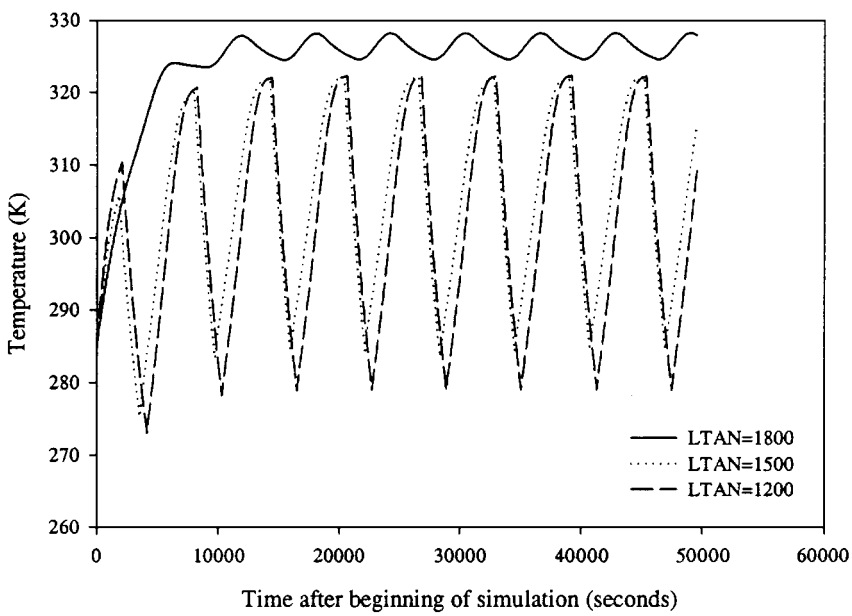

b) 1-g sphere

Fig. 4 Thermal modeling results.

curves, which correspond to debris with ascending nodes located at 1200 local time (LT), i.e., local noon, 1500 LT, and 1800 LT, i.e., local dusk. Consider the 57-g sphere in Fig. 4a. When the LT of the ascending node (LTAN) is 1800, the sphere never enters eclipse and gradually warms to a temperature of ~326 K. The small temperature fluctuation is a result of the variation in Earth-reflected sunlight over the course of an orbit. As the LTAN decreases, the droplet begins to undergo eclipse, and a saw-toothed pattern develops in the thermal history. At LTAN = 1500, the sphere's temperature varies between 302 and 313 K, whereas at LTAN = 1200 the temperature varies between 289 and 311 K. Because of the symmetry of this model about the Earth–sun line, the temperature of debris in orbits with ascending nodes at other LTs varies in the same fashion; therefore, this set of three orbits is representative of the temperature variation of the debris as a function of ascending node location. Note that the variation in temperature is a maximum for the orbit with LTAN = 1200; this is because the sphere spends more time in eclipse in this orbit than in any of the others, allowing it to cool to lower temperatures. Note that the temperature of the 57-g sphere never decreases below the freezing point of eutectic NaK, implying that the sphere remains in the liquid state.

The behavior of the 1-g sphere is presented in Fig. 4b. The less massive sphere undergoes larger temperature variations during its orbit, but its temperature remains well above the freezing point of eutectic NaK. The larger temperature variation is because the energy input scales as r^2 (area), whereas the thermal mass scales as r^3 (volume). Therefore, dT/dt varies as r^{-1} and is larger for smaller/less massive droplets.

The variation of the droplet temperatures as a function of altitude is presented in Table 1. The temperature of the droplets remain above 260 K at all relevant altitudes.

In Fig. 5, we present thermal history curves for the 11 anomalous debris orbits presented in Ref. 1; the orbital elements for the debris are presented in Table 2. Individual thermal histories are difficult to discern, but the envelope of the temperature variations is evident. None of the anomalous debris temperatures drop below 260 K. Therefore, we infer that the anomalous debris are likely to be liquid NaK droplets.

This model is not a high-fidelity calculation of the debris temperature. The calculation performed here is sufficient to demonstrate whether the temperature of the spheres lies near the freezing point of eutectic NaK; we have concluded that they do not. A discussion of the limitations of the model is useful. We assumed that the albedo of the Earth is a globally averaged constant with a value of 0.34. In reality, the albedo of the Earth is dependent on the reflective nature of the surface and the amount of cloud cover. The surface albedo is in turn dependent on the nature of the surface; water, snow, vegetation, and desert all reflect light differently. Cloud albedo is also dependent on the type and thickness of the cloud cover.[7] Obviously, the globally averaged albedo does not remain constant; Peixoto and Oort[7] suggest that it varies between 0.26 and 0.32 annually. A second issue related to albedo is that, for low-altitude objects, the debris temperature is dependent on the average albedo of the Earth scene, which is visible to it, not the albedo of the entire globe. This number can vary from ~0.25 to ~0.70 (Ref. 7). To address both of these issues, a test was run with the albedo set to 0.0 to determine how much the debris temperature decreases. For a droplet at 925-km altitude, 65-deg inclination, and LTAN = 1200, the temperature ranges from ~289 to 301 K, a 9–10-K decrease. For LTAN = 1800, the temperature decrease is ~3 deg. The debris temperature does not fall below the eutectic NaK freezing point even in the absence of Earth-reflected sunlight.

In our model we neglected the ~23-deg tilt of the Earth's rotation axis away from the normal to the ecliptic plane. The tilt will

Table 1 Thermal modeling results

Altitude, km	LTAN	Temperature, K	
		57-g sphere	1-g sphere
850	12	300–312	280–324
850	15	303–310	286–324
850	18	327–328	326–330
925	12	289–311	279–322
925	15	302–313	285–322
925	18	326	323–326
1000	12	297–309	277–320
1000	15	300–311	283–321
1000	18	323–325	323–327

Table 2 Orbital parameters for anomalous debris

Object no.	Inclination, deg	Eccentricity	Right ascension, deg	Semimajor axis R_E
81215	64.96	0.004	304.38	1.146
33562	65.04	0.004	77.291	1.146
33609	64.96	0.005	203.35	1.146
33612	64.97	0.005	187.93	1.146
33616	64.69	0.006	207.65	1.147
39969	64.69	0.006	222.31	1.147
39970	64.65	0.006	207.86	1.147
39971	64.96	0.004	300.13	1.146
39972	64.97	0.005	202.81	1.146
39973	65.05	0.004	86.32	1.146
39974	65.06	0.004	152.82	1.145

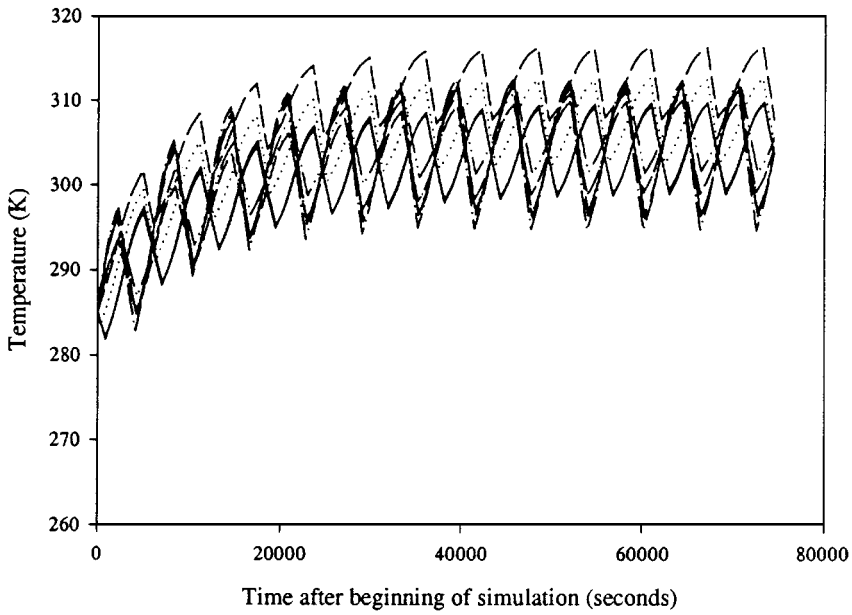

Fig. 5 Compilation of the modeled thermal histories for the debris objects listed in Table 2.

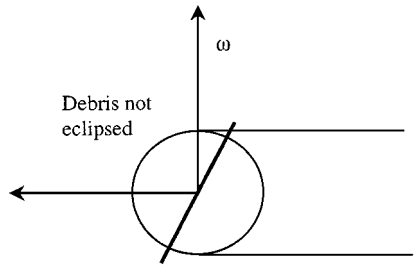

a) Debris orbit at the equinox

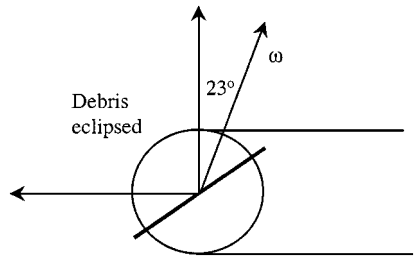

b) Debris orbit at northern hemisphere winter solstice

Fig. 6 Seasonal eclipsing of debris with LTAN = 1800.

cause a seasonal eclipsing of the debris and, thus, a seasonal effect in the temperature of the debris. Consider a NaK sphere with LTAN = 1800 (dusk terminator) and an orbital inclination of 65 deg. At the winter solstice, the Earth's axis is tipped ~23 deg away from the sun. This reduces the angle between the ecliptic and the orbit plane from 65 to 42 deg (Fig. 6a). The sphere will then be eclipsed during a portion of its orbit. For debris with LTAN = 0600 (dawn terminator), the debris can enter eclipse during southern hemisphere winter. This effect is simulated by reducing the orbital inclination in the model to 42 deg; the predicted temperature of the debris at 925-km altitude was reduced from 326 K to the range of 302–312 K (Fig. 6b). This is still well above the freezing point of eutectic NaK.

Finally, we note that the computed debris temperatures depend strongly on absorptivity and emissivity values. If these values are inaccurate, our conclusion that the debris are liquid could be incorrect. However, based on the available literature on the subject, we believe we have made a reasonable estimate of the absorptivity and emissivity values for NaK, and we conclude that the debris are probably in the liquid state.

Effect of Evaporation on Evolution of the Debris Orbits

Given that the anomalous debris are in the liquid state, the question of whether these droplets evaporate and the time scale over which evaporation occurs can have important implications for the orbital lifetime. The atmospheric drag force on the droplets depends on the ratio of projected area to mass. Loss of mass due to evaporation would lead to a change in the area-to-mass ratio and variation of the drag force on the debris. This could allow the debris to decay into heavily used orbits.

The flux of evaporating particles can be estimated from the principles of kinetic theory. Particles in the liquid with kinetic energies greater than the work necessary to move the particle from its initial position to infinity will escape into the surrounding space. This work function for the liquid can also be thought of as the latent heat of evaporation referred to a single particle. A minimum escape velocity for the particle can be derived from $mv^2/2 = U_0$, where U_0 is the latent heat of evaporation mentioned earlier. Then, estimation of the escaping flux is a simple matter of calculating the first moment of the liquid's velocity distribution function.

However, we were unable to obtain a value for the latent heat of evaporation for the NaK liquid, nor can we do any better than assuming a velocity distribution function for the droplet. Therefore, the assumption was made that the rate of evaporation is equal to the rate at which the vapor particles would strike the liquid if the liquid and the vapor were in equilibrium. This rate (kilograms per second) is

$$W = \kappa A_s P \sqrt{M/2\pi RT} \tag{10}$$

This is the maximum rate of evaporation.[14] We know of no measurements of the vapor pressure of the eutectic NaK system at the low temperatures that the droplets experience on orbit. Therefore, we adopt an evaporation theory that applies to binary alloys. The evaporation rate (kilograms per second) is slightly modified to account for the two different components. It is expressed as

$$W_i = \kappa_i A_s P_i^0 \gamma_i(x) N_i \sqrt{M_i/2\pi RT} \tag{11}$$

where i refers to a specific component (Na or K in this case). The mole fractions are expressed as

$$N_{\mathrm{Na}} = \left[\frac{(a-x)}{M_{\mathrm{Na}}}\right] \Bigg/ \left[\frac{(a-x)}{M_{\mathrm{Na}}} + \frac{(b-y)}{M_{\mathrm{K}}}\right] \tag{12a}$$

$$N_{\mathrm{K}} = \left[\frac{(b-y)}{M_{\mathrm{K}}}\right] \Bigg/ \left[\frac{(a-x)}{M_{\mathrm{Na}}} + \frac{(b-y)}{M_{\mathrm{K}}}\right] \tag{12b}$$

Note that as time passes and more of each element evaporates from the system, the mole fractions change (as do the atomic fractions of Na and K and the activity coefficient γ). Determination of the time scale for evaporation of the droplets required numerical solution of the following coupled differential equations:

$$\frac{\mathrm{d}x}{\mathrm{d}t} = W_{\mathrm{Na}}(x, y), \qquad \frac{\mathrm{d}y}{\mathrm{d}t} = W_{\mathrm{K}}(x, y) \tag{13}$$

To calculate evaporation rates, the vapor pressures of Na and K and the activity coefficients must be known. The vapor pressures of Na and K at low pressures and temperatures ranging from their normal melting points (371 K for Na and 337 K for K) to ~463 K are given by the following relations:

$$\log P_{\mathrm{Na}} = 8.08 - (5479/T), \qquad \log P_{\mathrm{K}} = 7.56 - (4587/T) \tag{14}$$

where P is in torr and T is in degrees Kelvin.[8] The activity coefficients are given in Table 3.[15]

As in the last section, droplets with masses of 1 and 57 g were considered. To facilitate the calculation of evaporation rates, the droplets were assumed to maintain an average temperature over an orbit, and three temperatures were considered: 300, 330, and 280 K. These temperatures correspond to debris in orbits that are eclipsed, orbits that are not eclipsed, and an arbitrary low temperature, respectively.

For eutectic NaK, the droplets are 77.8% K by mass; therefore, the 57 g (1 g) droplet initially contains 44.346 g (0.778 g) of K and 12.654 g (0.222 g) of Na. The initial atomic fraction of Na in the droplets was 0.3267 (32.67% of the atoms in the droplets were Na atoms); this was used to interpolate the initial activity coefficients for the systems. The initial vapor pressures were calculated using Eq. (14), and it is assumed that the vapor pressures do not change as the elements evaporate. We also assume that the composition

Table 3 Activity coefficients for liquid NaK at 298.15 K

Atomic fraction Na	$\gamma_{\mathrm{Na}}(\pm 0.06)$	$\gamma_{\mathrm{K}}(\pm 0.06)$
0.0	3.00	1.00
0.1	2.43	1.01
0.2	2.02	1.05
0.3	1.71	1.11
0.4	1.49	1.19
0.5	1.29	1.29
0.6	1.19	1.49
0.7	1.11	1.71
0.8	1.05	2.02
0.9	1.01	2.43
1.0	1.00	3.00

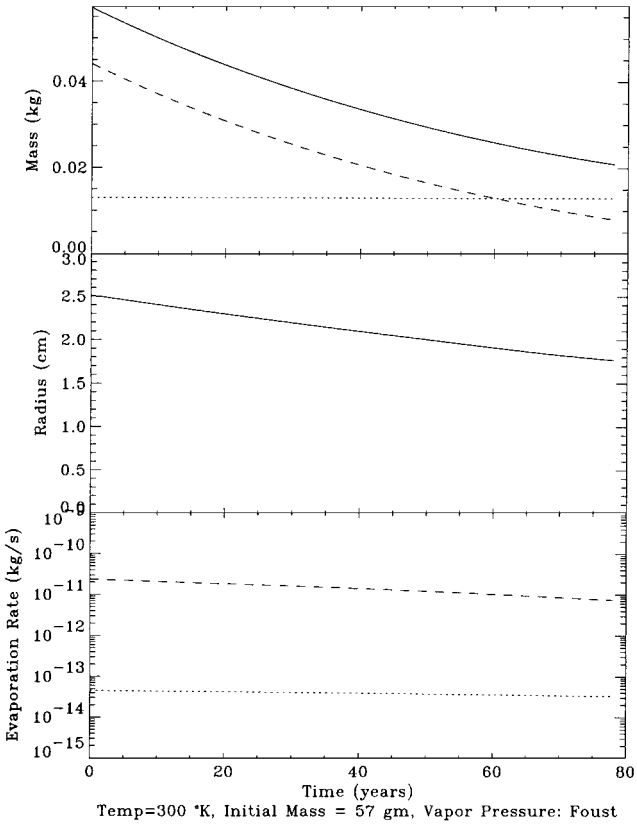

Fig. 7 Results of the evaporation modeling for the 57-g droplet: – –, potassium component; · · ·, sodium component; and —, sum of the two components.

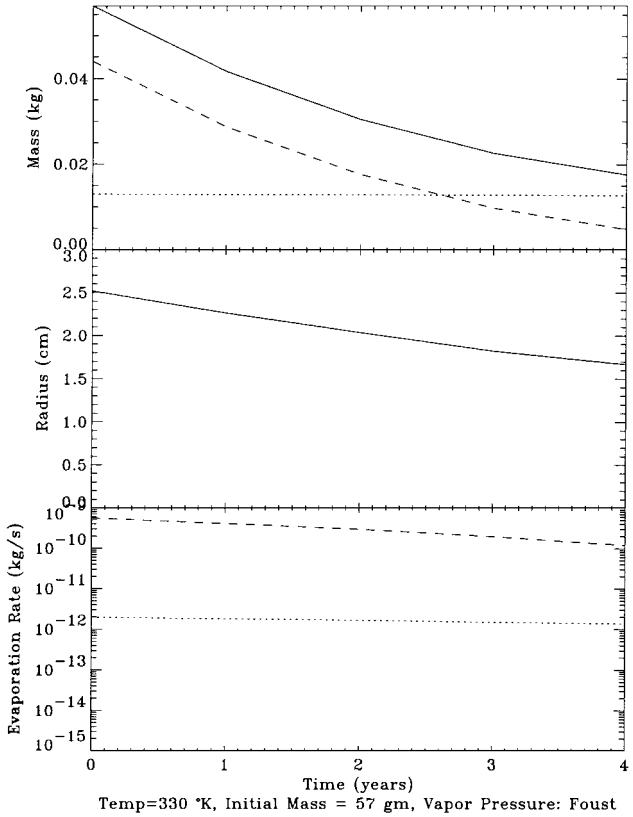

Fig. 8 Evaporation results for the 57-g droplet at 330 K in the same format as Fig. 7.

of the droplets remains uniform. These two important assumptions will be discussed subsequently. Note also that the vapor pressure formulas are being applied at temperatures below which they are deemed applicable because the NaK system is still liquid at these temperatures. Given these initial conditions, Eqs. (13) are integrated using a time step of 86,400 s. The initial evaporation rates are so small (4.03348×10^{-12} kg/m^2-s for Na and 4.21491×10^{-9} kg/m^2-s for K) that the relatively large time step is acceptable. It should be noted that the simulation is stopped if a phase transition is brought on by the changing composition of the droplet.

Figure 7 presents the results of the evaporation simulation for the 57-g droplet at 300 K. The simulation covered ~79 years. The mass loss from the droplet in total and for the individual components is shown in the top panel. The Na component evaporates very little over the course of the simulation. The K component evaporates at a relatively rapid pace, and after ~79 years the composition of the drop has changed sufficiently to raise the melting point above 300 K, i.e., solidification begins. The second panel shows the change in the radius of the droplet; the radius decreases by ~0.75 cm during the simulation. The third panel shows the evaporation rates for each component of the alloy. The rates slow as the elements evaporate from the system and the mole fractions decrease. The effect of the phase transition on the system is discussed subsequently.

Figure 8 shows the results for the 57-g droplet at a temperature of 330 K. In this case, the potassium evaporated rapidly, and the droplet began solidifying after ~4 years. This rapid evaporation can be explained by examination of Eq. (14); a 30-deg increase in temperature increases the initial potassium vapor pressure from 2.475×10^{-6} to 6.075×10^{-5} Pa, a factor of ~24 increase. The evaporation rate is directly proportional to the vapor pressure; therefore, it also increases by a factor of ~24. This demonstrates that the evaporation rate is extremely sensitive to the value of the vapor pressure.

Figure 9 shows the results for the 1-g droplet at a temperature of 300 K. Sufficient potassium evaporates from this system in ~20 years for solidification to begin, slightly faster than for the larger droplet. Considering that the evaporation rate is lower (third panel of Fig. 9), this result is counterintuitive. However, for a given period of time, the mass loss per unit mass ($\Delta m/m$) is larger for smaller droplets ($\Delta m/m \sim r^{-1}$), causing the smaller droplets to evaporate more quickly. The radius of the droplet decreases from 6.5 to ~4.5 mm over the course of the simulation.

Table 4 Simulation results

Initial/final mass, g	Temperature, K	Initial/final radius, cm	Phase transition, yr
57.0/28.36	280.0	2.507/1.975	634.26
57.0/20.88	300.0	2.511/1.767	78.10
57.0/16.05	330.0	2.518/1.615	4.466
1.0/0.497	280.0	0.652/0.514	164.36
1.0/0.366	300.0	0.653/0.460	20.24
1.0/0.281	330.0	0.655/0.420	1.15

Figure 10 shows the results for the 1-g droplet at 330 K. Sufficient potassium evaporates from the system in ~1 year to induce solidification. The radius of the droplet decreased to ~4 mm. Table 4 presents the results for all of the simulations.

Table 4 shows that the NaK droplets always go through a phase transition that is induced by the change in composition as they evaporate. In Fig. 11, the phase diagram for NaK is presented. The eutectic mixture (the starting point in the simulations) is denoted. The melting point for the various mixtures is marked by the top line in the plot (liquidus). As the droplet evaporates at constant temperature, the fraction of K decreases relatively rapidly. Eventually, the melting point rises above the temperature maintained in the simulation, and solidification of the liquid begins. For the temperature range considered in this paper, the NaK changes to a mixture of liquid and solid when the liquidus is crossed. The composition of the liquid (solid) is given by the composition at which the constant temperature line intersects the liquidus (solidus). For example, at 300 K, when the K mass fraction decreases to ~40%, the liquid has a composition of ~40% K and ~60% Na by mass/weight, whereas the forming solid has a composition of ~6% K and ~94% Na by mass/weight. The relative compositions of this liquid/solid mixture will not change unless the temperature is changed; for additional evaporation of the K to occur, the temperature must be increased.[16,17] The simulation

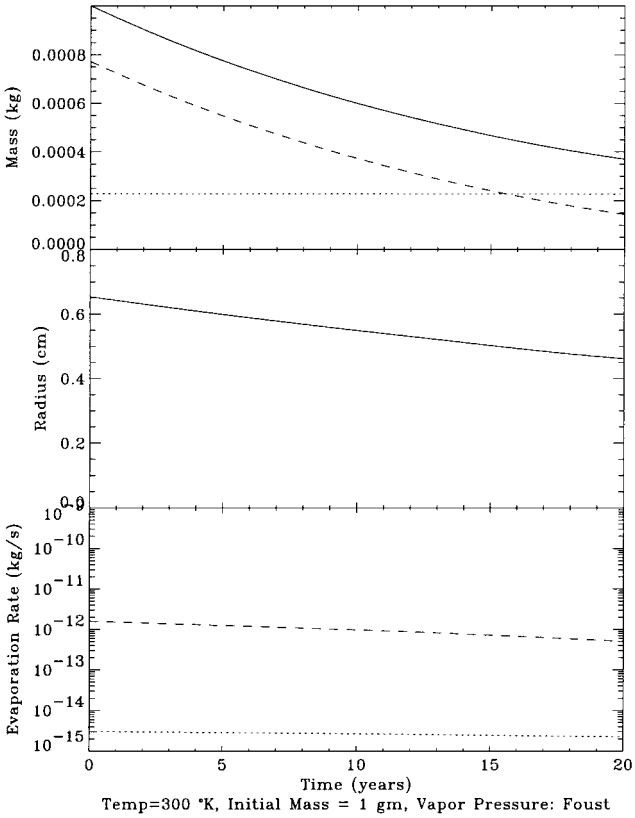

Fig. 9 Evaporation results for the 1-g droplet at 300 K in the same format as Fig. 7.

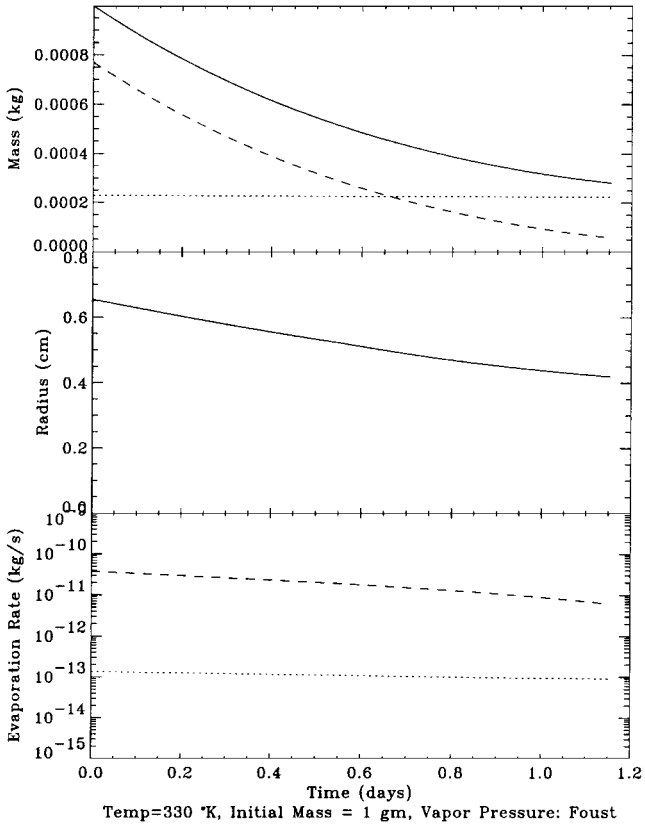

Fig. 10 Evaporation results for the 1-g droplet at 330 K in the same format as Fig. 7.

Table 5 Simulation results for equalized pressures

Initial/final mass, g	Temperature, K	Initial/final radius, cm	Phase transition, yr
57.0/26.54	280.0	2.507/1.933	13,354.12
57.0/18.05	300.0	2.511/1.724	12,255.03
57.0/43.79	330.0	2.518/2.333	352.55
1.0/0.465	280.0	0.652/0.503	3,460.61
1.0/0.317	300.0	0.653/0.448	3,175.79
1.0/0.166	330.0	0.655/0.365	4,610.94

was stopped at the phase transition because very little is known about how the droplet solidifies or the differences in evaporation from the liquid and solid alloys. Examination of Tables 4 and 5 show that, once solidification begins, anywhere from 15 to 50% of the droplet's original mass still remains. Therefore, complete evaporation of the droplets could take much longer than the time scales presented.

We noted earlier that the evaporation rates are very sensitive to the value of the vapor pressure(s); therefore, an assessment of the accuracy of the vapor pressure values given by Eq. (14) is desirable. This is difficult because we have extrapolated vapor pressure formulas for liquid Na and K down to temperatures below the freezing points of the individual elements. However, because the elements remain in the liquid state while in solution, and there is no direct measurement of the evaporation rate for NaK, this appears to be the only appropriate course of action. We can crudely estimate the uncertainty in the vapor pressure values by comparing extrapolations of the vapor pressure values derived by various researchers.[18] These comparisons are presented in Figs. 12 (Na) and 13 (K). At 300 K, the sodium vapor pressure agrees to within one to two orders of magnitude, with the value quoted in Eq. (14) being among the higher values. The potassium vapor pressure values agree to within an order of magnitude at 300 K, with the value quoted by Eq. (14) being the lowest value. Thus, our original calculation may prove to be a lower limit on the evaporation lifetimes. However, we choose not to calculate evaporation lifetimes using the higher potassium vapor pressures for reasons to be described.

Two additional assumptions used in this model may significantly affect the calculated evaporation rates. The first assumption is that of a constant vapor pressure value in equilibrium with the droplet. For potassium, the equilibrium vapor pressure at all temperatures considered here is significantly larger than the ambient atmospheric pressure at the altitude of the debris ($P_{atm} \sim 10^{-8}$ Pa at 925 km).[19] It seems unlikely that the potassium vapor pressure around the droplet would attain levels ~20–6000 times that of the neutral atmosphere; the pressure gradient force would cause the potassium atoms to diffuse away from the droplet. Except at 330 K, sodium vapor pressures remain well below atmospheric pressure. If we assume that the potassium atoms diffuse away from the droplet, the evaporation of the droplets would be slowed. To estimate the difference in evaporation rates, we conducted a series of model runs in which vapor pressures above the ambient atmospheric pressure were reduced to 10^{-8} Pa to simulate the outflow induced by the pressure gradient. Note that the sodium vapor pressures at the lower temperatures were not increased to remove the pressure gradient, as this would imply a second source of sodium atoms; however, at 330 K, the sodium vapor pressure was decreased to 10^{-8} Pa. The results are presented in Table 5 and should be considered crude estimates, perhaps correct only in order of magnitude.

The second assumption, uniform composition of the droplet, implies that there is a process on orbit that continually mixes the droplet as the components evaporate. In the event that there is no mixing, only the potassium near the surface of the droplet would evaporate quickly. After this potassium evaporates, the droplet might be surrounded by a thin sodium shell, which would evaporate at a much slower rate. This effect would also slow the evaporation of the droplets, but the effect may be minimal because the droplets are mostly potassium in the early stages of evaporation.

For droplets in certain orbits, the temperature varies as the droplet passes through sunlight and shadow; we assumed that the droplets maintained a constant temperature for computational ease. The preceding discussion has shown that the evaporation rate of the droplets is sensitive to their temperature. The effect on the evaporation rate of allowing the temperature of the droplets to vary as they evaporate was estimated by calculating the amount of material that evaporated

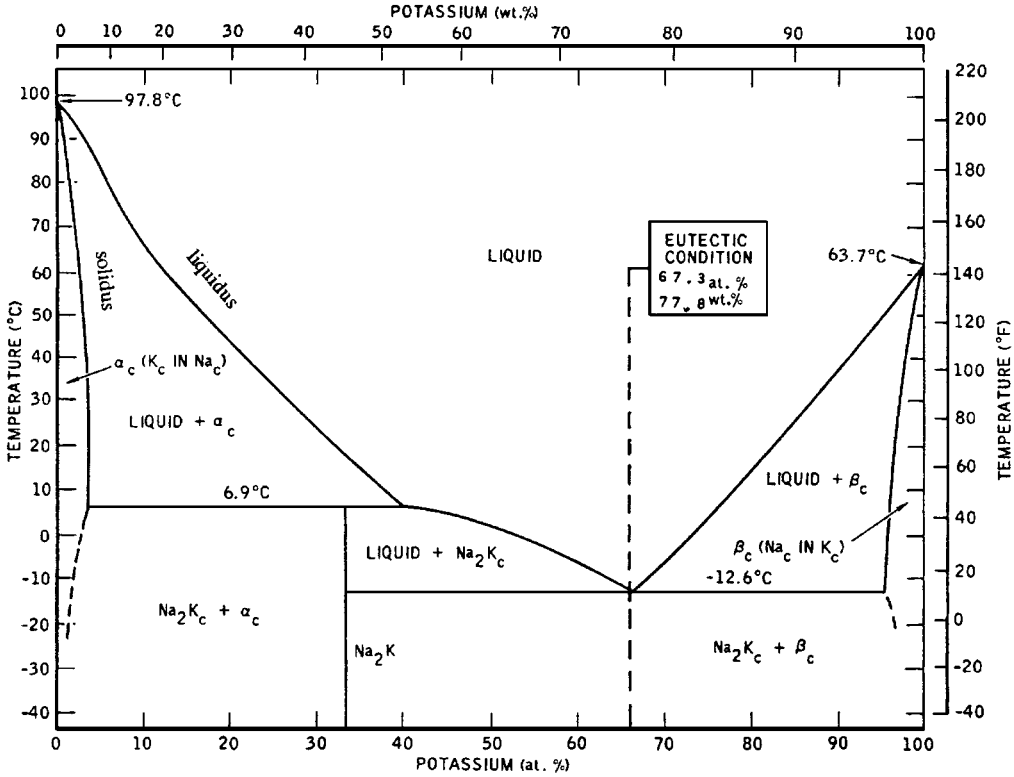

Fig. 11 NaK phase equilibrium diagram where phase is displayed as a function of temperature and percentage of potassium in the mixture. Adapted from Ref. 8.

from the droplets over the course of one orbit. In one case the temperature was allowed to vary, and in the other, the temperature was held fixed at the average temperature over the orbital cycle (~303 K for both droplets). It was found that for the 57-g droplet, only 5.32×10^{-10} kg evaporated when the temperature varied in a realistic fashion during the orbit, whereas 4.64×10^{-8} kg evaporated when the temperature was held constant. The 1-g droplet behaved in the opposite manner; 9.86×10^{-11} kg evaporated when its temperature was allowed to vary compared with 3.16×10^{-11} kg when the temperature was held constant. The reason for this is that the temperature variation for the smaller droplet is larger over the course of an orbit, as shown earlier. It reaches higher temperatures than a 57-g droplet in the same orbit and evaporates more quickly.

We stopped the simulation when the droplets began to solidify due to a lack of information concerning the evaporation of mixed liquid/solid state. Evaporation of a solid (sublimation) at constant temperature requires an amount of heat (per mole of substance) equivalent to the sum of the latent heats of fusion and vaporization at that temperature. Evaporation of a liquid at the same temperature requires an amount of heat (per mole) equivalent to the latent heat of vaporization at that temperature. We expect that solid will evaporate at a slower rate because the amount of energy required to liberate atoms is larger. Given the correct vapor pressures, the evaporation lifetimes could be computed using the same methods we employed. However, we know of no measurements of the vapor pressures for solid sodium and potassium.

Ultimately, we wish to compare the calculated evaporation lifetime with the time scale for decay of the debris into the atmosphere. We have estimated the length of time these droplets will spend on orbit using Ref. 20 (Figs. 12 and 13).[19] These lifetimes assume a ballistic coefficient C_D of 2.2 for the spheres, an atmospheric model representing an average amount of solar activity, and the initial area-to-mass ratios used in this paper. The lifetime estimates are good only to no better than ~20% and may be good to only a factor of ~2. They are presented in Table 6. Comparison of these lifetimes with the time scales presented in Table 5 suggests that it will take much longer for the droplets to evaporate significantly than it will for their orbits to decay. Previous work[2] indicates that 1-cm-diam NaK spheres at ~273 K ($m = 0.46$ g) and 950-km altitude would decrease in diameter due to evaporation at a linear rate over hundreds

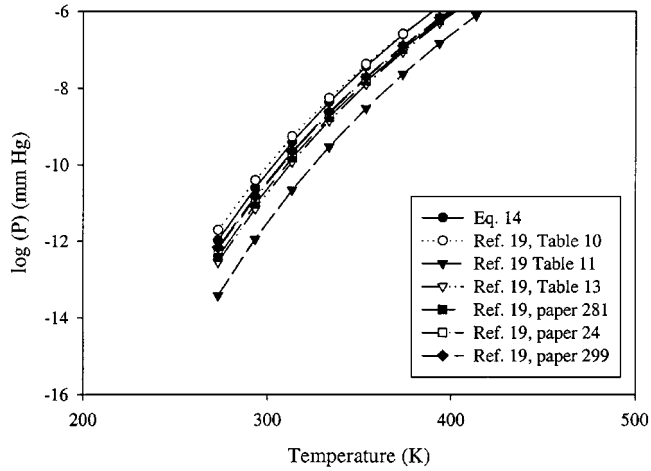

Fig. 12 Comparison of sodium vapor pressure values extrapolated from the results of various researchers; Eq. (14) is represented by the solid line with filled circles.

Table 6 Approximate orbital lifetimes of NaK droplets

Altitude, km	Lifetime, yr	
	$m = 57$ g	$m = 1$ g
850	172.8	45.2
925	288.0	75.3
1000	576.0	150.6

of years, but would reenter the atmosphere in ~80 years. This orbital lifetime is in approximate agreement with our lifetime estimate for a 1-g droplet. Russian work quoted in Ref. 2 indicates that 1-cm spheres at a temperature of 293 K would evaporate to 0.7 cm in ~100 years and is apparently consistent with the NASA calculations. We note that these results are roughly consistent with the results presented in Table 4 derived using the maximum evaporation rates. It does not appear that any previous work has allowed for phase transitions to occur in the droplet.

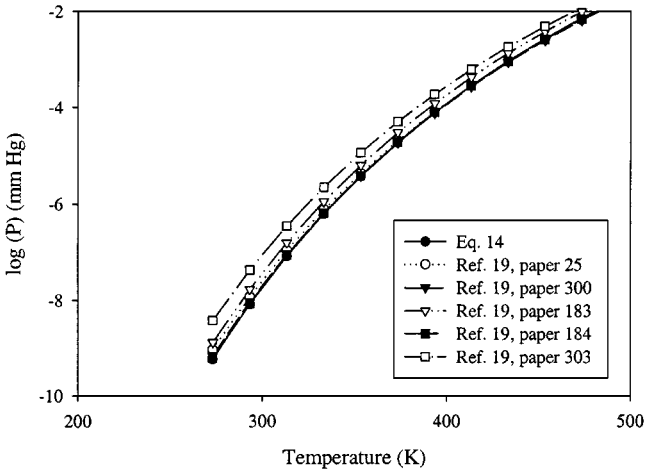

Fig. 13 Comparison of potassium vapor pressure values extrapolated from the results of various researchers.

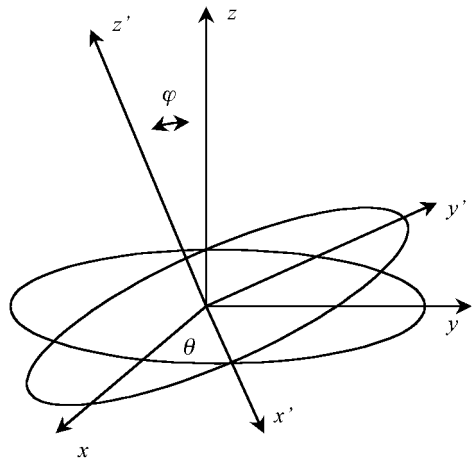

Fig. A1 Relative orientation of reference and debris (primed) coordinate systems.

Conclusions

A simple thermal model was constructed to facilitate characterization of an anomalous orbital debris population believed to be liquid NaK reactor coolant that leaked from Soviet RORSATs. It was found that spherical debris composed of eutectic NaK that lie in circular orbits in the altitude range of 850–1000 km are always in a liquid state. We note that this conclusion is dependent on the veracity of the estimate for the optical properties (α and ε) of eutectic NaK.

Given that the debris are in the liquid state, we also estimated the time scale for evaporation of NaK and compared it with the orbital lifetime. We constructed a model for the evaporation of a binary alloy and applied it to eutectic NaK droplets with various masses and temperatures. We have placed wide bounds on the evaporation lifetimes of the droplets ranging from just over 1 year to ~13,000 years. We caution that evaporation lifetime refers to the length of time that passes before the droplet begins to solidify. We did not carry the simulation past this point due to uncertainties regarding how the alloy evaporates during and after the solidification process. Thus, the time scales presented may represent only a fraction of the time required for the droplet to completely evaporate. We calculated the lifetimes using maximum evaporation rates (resulting in minimum lifetimes) and with what we consider to be more realistic evaporation rates by adjusting the vapor pressure of the two elements. The evaporation lifetimes calculated using the maximum evaporation rates, i.e., the higher value for the potassium vapor pressure, are in rough agreement with previous work by NASA and Russian researchers, but we believe many additional factors influence the evaporation rate, slowing it significantly. In conclusion, it seems likely that the evaporation lifetimes of these droplets range from at least ~3000–4000 years for the 1-g (6.5-mm radius) droplets to at least 12,000–13,000 years for the 57-g (2.5-cm radius) droplets. In this case, the lifetime on orbit would be controlled by orbital decay and not by evaporation. However, there is significant uncertainty in these results, and measurement of the evaporation rate of NaK may prove useful.

Appendix: Coordinate Systems

Reference Inertial Coordinate System

This coordinate system is the one in which the energy inputs to the debris object are calculated. The origin is at the center of the Earth and the x axis points toward the sun. The z axis is aligned with the Earth's rotation axis and is assumed to be normal to the ecliptic plane at all times (axial tilt of the Earth equal to 0 deg). The y axis completes the right-handed system. The x–y plane lies in the ecliptic and also corresponds to the Earth's equatorial plane.

Debris Orbit Plane Coordinate System

We denote the debris coordinate system as the primed coordinate system. With respect to the reference coordinate system, any orbital plane coordinate system can be represented by two rotations. Begin with the two systems coaligned ($x = x'$, $y = y'$, $z = z'$). Rotate the primed system about the z axis counterclockwise by an angle α. Next rotate the primed system about the x' axis by an angle β. The angle β represents the inclination of the orbit, and the intersection of the two orbital planes represents the location of the ascending node. The local time location of the ascending node is characterized by α. The coordinate systems are shown in Fig. A1.

The transformation from the primed coordinate system to the reference system is

$$\bar{r} = A \cdot \bar{r}' \tag{A1}$$

$$A = \begin{bmatrix} \cos\theta & -\sin\theta\cos\varphi & \sin\varphi\sin\theta \\ \sin\theta & \cos\varphi\cos\theta & -\sin\varphi\cos\theta \\ 0 & \sin\varphi & \cos\varphi \end{bmatrix}$$

Sun-Centered Coordinate System

A third system is used briefly to determine whether the debris is in eclipse. This is a right-handed system, which has its origin at the center of the sun. The x axis points from the center of the sun to the center of the Earth, the z axis is aligned with the solar rotation axis (normal to the solar ecliptic), and $y = z \times x$. When the eclipse algorithm is implemented, the debris position vector must be transformed to this system to calculate the vector $\boldsymbol{X}$. This is very simple; the transformation is $x'' = -x$, $y'' = -y$, and $z'' = z$. The unprimed system refers to the reference coordinate system.

References

[1] Sridharan, R., Beavers, W., Gaposchkin, E. M., Lambour, R., Kansky, J., and Stansbery, E., "Radar and Optical Characterization of an Anomalous Orbital Debris Population," *Journal of Spacecraft and Rockets*, Vol. 36, No. 5, 1999, pp. 719–725.

[2] Kessler, D. J., Matney, M. J., Reynolds, R. C., Bernhard, R. P., Stansbery, E. G., Johnson, N. L., Potter, A. E., and Anz-Meador, P. D., "A Search for a Previously Unknown Source of Orbital Debris: The Possibility of a Coolant Leak in Radar Ocean Reconnaissance Satellites," 48th International Astronautical Congress, Paper IAA-97-IAA.6.3.03, Turin, Italy, Oct. 1997.

[3] Bennett, G., "A Look at the Soviet Space Nuclear Power Program," *Proceedings of the 24th Intersociety Energy Conversion Engineering Conference*, Vol. 2, Inst. of Electrical and Electronics Engineers, New York, 1989, pp. 1187–1194.

[4] Miller, R. R., *Liquid Metals Handbook, Sodium (NaK) Supplement*, edited by C. B. Jackson, Atomic Energy Commission and Dept. of the Navy, 1955, pp. 1–50.

[5] Cunningham, F. G., "Earth Reflected Solar Radiation Input to Spherical Satellites," *ARS Journal*, Vol. 32, No. 7, 1962, pp. 1033–1036.

[6] Wolfe, W. L., and Zissis, G. J., *The Infrared Handbook*, 1st ed., Office of Naval Research, Washington, DC, 1978, pp. 15–55.

[7] Peixoto, J. P., and Oort, A. H., *Physics of Climate*, 1st ed., American Inst. of Physics, New York, 1992, pp. 118, 119.

[8] Foust, O. J. (ed.), *Sodium NaK Engineering Handbook*, 1st ed., Vol. 1, Gordon and Breach, New York, 1972, pp. 1–59.

[9]Meshcheryakov, S. A., "Physical Characteristics of Alkaline Metals and Behavior of Liquid Metal Coolant Droplets in Near-Earth Orbits," *Proceedings of the Second European Conference on Orbital Debris*, ESA, Noordwijk, The Netherlands, 1997, pp. 257–259.

[10]Morgan, R., "The Optical Constants of Sodium-Potassium Alloys," *Physical Review*, Vol. 20, No. 3, 1922, pp. 203–213.

[11]Jackson, J. D., Tong, D. K. W., Barnett, P. G., and Gentry, P., "Measurement of Liquid Sodium Emissivity," *Nuclear Energy*, Vol. 26, No. 6, 1987, pp. 387–392.

[12]Hattori, N., Takasu, H., and Iguchi, T., "Emissivity of Liquid Sodium," *Heat Transfer, Japanese Research*, Vol. 13, No. 1, 1984, pp. 30–40.

[13]Kamiuto, K., "Radiative Properties of Liquid Potassium," *Journal of Nuclear Science and Technology*, Vol. 23, No. 4, 1986, pp. 372–374.

[14]Ohno, R., "Kinetics of Evaporation of Various Elements from Liquid Iron Alloys Under Vacuum," *Liquid Metals*, 1st ed., Marcel Dekker, New York, 1972, pp. 37–80.

[15]Hultgren, R. R., *Selected Values of Thermodynamic Properties of Metals and Alloys*, 1st ed., Wiley, New York, 1963, pp. 829, 830.

[16]Gordon, P., *Principles of Phase Diagrams in Materials Systems*, 1st ed., McGraw–Hill, New York, 1968, pp. 131–161.

[17]Guy, A. G., and Hren, J. J., *Elements of Physical Metallurgy*, 1st ed., Addison–Wesley, Reading, MA, 1974, pp. 285–310.

[18]Nesmeyanov, A. N., *Vapor Pressure of the Chemical Elements*, 1st ed., Elsevier, New York, 1963, pp. 128–143.

[19]Jursa, A., *Handbook of Geophysics and the Space Environment*, 2nd ed., U.S. Air Force Geophysics Lab., Hanscom AFB, MA, 1985, pp. 14-3, 14-4.

[20]King-Hele, D., *Satellite Orbits in an Atmosphere: Theory and Applications*, 1st ed., Blackie and Son, London, 1987, pp. 258–263.

A. C. Tribble
Associate Editor